RESEARCH ARTICLE Indian Journal of Animal Research, Volume 58 Issue 12: 2146-2153 (December 2024)

Lumpy Skin Disease Detection in Cattle by a Robust Approach using Advanced Convolutional Neural Networks

Ahmad Ali AlZubi[1]

10.18805/IJAR.BF-1793

ABSTRACT

Background: Lumpy skin disease (LSD) is a significant health concern for cattle globally and poses economic threats by affecting various aspects of cattle health. Integrating artificial intelligence (AI) and machine learning (ML) with visual inspections and biosensor data has shown promise in enhancing disease detection and diagnosis. The present study harnesses the potential of Convolutional Neural Networks (CNN) and image processing for detecting LSD.

Methods: Using images from the agricultural landscape, this study highlights the significance of convolutional neural networks that identify the lumpy skin disease (LSD) in animals. Images are categorized into two groups: LSD (infected skin) and non-LSD (normal skin). This is achieved by applying a deeply designed deep learning model carefully built to fulfill this particular need. Evaluation metrics assess the model's performance, including accuracy, loss and a confusion matrix.

Result: A CNN-based model trained for 50 epochs to classify skin conditions, achieved an 86.54% accuracy. The study underscores the potential of CNN in early LSD detection, paving the way for practical applications in veterinary medicine. Future work involves addressing dataset limitations, refining model parameters, reducing image noise, exploring different feature extraction methods and investigating additional animal skin conditions.

Key words: Cattle, Convolutional neural network, Image processing, Lumpy skin disease, Transfer learning.

INTRODUCTION

Cattle often suffer from skin diseases such as Lumpy Skin Disease (LSD), Dermatophilosis (Streptothricosis), Dermatophytosis (ringworm) and Bovine papillomatosis (warts) (Tageldin *et al*., 2014; Scott, 2018; Rojas-Anaya *et al*., 2016). These conditions pose a significant problem, leading to the rejection of skin and hide products due to poor quality caused by these diseases (Bekele, 2017). One of the emerging skin diseases that is posing significant health concerns for cattle worldwide is Lumpy Skin Disease (LSD). Lumpy skin disease (LSD), which is prevalent in Africa and Turkey, has been rapidly spreading to other parts of the world, including Europe and Asia (Bekele, 2017; Whittle *et al*., 2023; Amin *et al*., 2021). This highly contagious viral disease poses a significant threat to cattle globally. LSD is caused by a virus (genus - *Capripoxvirus*) and has the potential to impact economic value by affecting meat and milk production, hide quality, draft power of animals and reproductive efficiency, leading to issues such as abortion and infertility (Gupta *et al*., 2020; Whittle *et al*., 2023). The disease is characterized by the formation of nodules or lumps on the skin, mucous membranes and internal organs of infected cattle. The disease may spread via a number of different routes. Through polluted settings, fomites, or vectors, there is environmental and indirect transmission. Tick cell line cultivation in vitro could help in dispersion, which might result in airborne spread. Conversely, direct contact includes the spread *via* contaminated medical equipment and aerosols, which may present serious dangers in medical environments. The term vertical transmission refers to the disease's transfer from mother to child *via* the uterus. Additionally, vaccinated cows may sometimes discharge milk with vaccine virus, which would further complicate the dynamics of transmission. Furthermore, the disease might be expelled in the semen of cows, which increases the possibility of vertical transmission. Moreover, live animals, unsterilized animal products, or contaminated objects may transmit the disease over vast distances, which emphasizes the need for strict biosecurity measures to stop its spread.

A conclusive diagnosis of skin diseases requires a systematic approach that involves a complete analysis of medical history, a comprehensive physical examination and appropriate diagnostic tests. To diagnose LSD, clinicians typically rely on recognizing typical clinical signs, using differential diagnosis and employing various laboratory techniques. These techniques include serological tests, polymerase chain reaction (PCR), indirect fluorescent antibody technique and electron microscopy

[1]Department of Computer Science, Community College, King Saud University, Riyadh, Saudi Arabia.

Corresponding Author: Ahmad Ali AlZubi, Department of Computer Science, Community College, King Saud University, Riyadh, Saudi Arabia. Email: aalzubi@ksu.edu.sa
Orcid id: https://orcid.org/0000-0001-8477-8319

How to cite this article: AlZubi, A.A. (2024). Lumpy Skin Disease Detection in Cattle by a Robust Approach using Advanced Convolutional Neural Networks. Indian Journal of Animal Research. 58(12): 2146-2153. doi: 10.18805/IJAR.BF-1793.

Submitted: 27-03-2024 **Accepted:** 21-06-2024 **Online:** 17-07-2024

(Gari *et al*., 2008; Sharawi and Abd El-Rahim, 2011; Baselli *et al*., 2023). They are important, but they are not ideal for early disease screening. For example, serological assays are time-consuming and prone to potential cross-reactivity with other poxviruses (Zeedan *et al*., 2019). On the other hand, molecular methods such as PCR, though less time-consuming, require isolated DNA and high-end pieces of equipment and well-established setups not suitable for on-site investigation (Vidic *et al*., 2017). Hence, alternatives like biosensors are being developed which combine a biological component such as enzymes, antibodies, or nucleic acids with a detector to generate measurable signals (for detection) for target analytes. Specifically, PCR biosensors detect LSD viral DNA, while immunosensors use antibodies against LSD viral antigens for rapid and specific virus detection, facilitating early diagnosis and disease control in cattle populations (Li *et al*., 2021; Xiong *et al*., 2022). However, for timely and prompt measures taken to prevent the spread of disease to other animals and reduce economic loss, early detection of the disease is important. Typically, early screening involves a thorough physical examination of an animal's hair coat and skin under strong lighting (Moriello, 2022). However, this process requires extensive human experience and expertise, which can lead to subjective errors.

Recently, artificial intelligence and machine learning (ML) have been integrated with the information obtained from visual inspections and biosensor data to enhance the efficiency of disease diagnosis and subsequent treatments (AlZubi, 2023; Cho, 2024; Neethirajan and Kemp, 2021; Kadian *et al*., 2023; Kumar *et al*., 2023; Wasik and Pattinson, 2024). The advent of image processing has presented an excellent opportunity for the identification of skin lesions, lumps, nodules or any other manifestation of skin diseases (Srinivasu *et al*., 2021; Affolter *et al*., 2023). In the case of LSD, the early stages of infections which are mild and may be difficult to distinguish (though the severe cases can be easily recognized) entail the utilization of artificial intelligence for disease detection with better accuracy (Tupparainen *et al*., 2017; Li *et al*., 2021; Rashid *et al*., 2018). The procedure is sped up with the use of image processing, which extracts distinguishing characteristics from the images (Nachbar *et al*., 1994). The study by Dofadar *et al*. (2022) used ten ML classifiers. The RF Classifier and Light Gradient Boosted Machine Classifier outperformed others, achieving a remarkable F1 score of 98%. Genemo (2023) employed CNN to develop a system trained on a Cattle's LSD dataset by extracting features on the basis of ABCD rule of dermatoscopy which included conditions like "asymmetry (A), border (B), colour (C) and differential structure (D)".

While existing studies demonstrate the potential of machine learning for both predicting and detecting lumpy skin disease, there remains a dearth of research utilizing image-based AI for direct lesion identification. To address this gap, this present study introduces a novel CNN model employing transfer learning for accurate lumpy skin disease detection in cattle, aiming to advance rapid diagnosis and intervention in resource-limited settings.

MATERIALS AND METHODS

Image dataset

For the CNN model, a well-labeled, fine dataset of animal images with normal and lumpy skin disease was collected and divided into two groups representing the diseased and normal conditions. The dataset contained 1,023 images, including different categories such as age, breed and severity of disease (Table 1). Data for this study was collected with the help of specialists in the field of cattle farming. Specifically, the images in this collection included both LSD and non-LSD skin images and a sufficient number of images were kept in each category. The lumps or nodules on the skin of the animal were the main clinical indications for this disease (Fig 1). These could also be seen in the skin, cups and mucous membranes and they could range in size (Datten *et al*., 2023). The dataset was split into a training set and a validation set with an 80:20 ratio, where 80% of the data was used for training and 20% was used for validation.

Table 1: Details of animals.

Breed	Total animal number	Age (yrs)	Sex	Severity of lesions
Vechur	250	1-3	90% female and 10% male	Mild, moderate and severe
		4-8		
		8 to more		
Swiss Holstein	280	1-3	90% female and 10% male	
		4-8		
		8 to more		
Jersey	215	1-3	Female only	
		4-8		
		8 to more		
Ponwar	278	1-3	90% female and 10% male	
		4-8		
		8 to more		

Data pre-processing

The first step in the image-based ML technique involves the input of a dataset, known as the pre-processing stage, which helps in the optimal preparation of images by removing unwanted noise (Salvi *et al.*, 2021). To keep images identical, they were resized to 256 × 256 pixels. This is important because the model needs uniformly sized input images to analyze data as efficiently as possible. This was followed by normalization where each image is transformed into a set of pixel values that align more closely with familiar or standard ranges (Hosakoti *et al.*, 2021). For this, each pixel value in an image was divided by 255, the maximum value for its bit-depth, to ensure that the pixel values range between 0 and 1 (Johnson *et al.*, 2019). Image normalization is a common procedure in image processing that alters the range of pixel intensity values. Improved integration during the model's training is made possible by this normalization. Each picture was then labelled with the appropriate health category. These training and test datasets allowed for the identification of two classes: LSD and non-LSD skin images.

Data augmentation

The data augmentation technique is used to generate new images based on the existing dataset to increase the diversity and variability of the dataset. Images may be shifted, rotated randomly, zoomed in and flipped vertically or horizontally during this augmentation process. The employment of data augmentation is essential in increasing the model's capacity to generalize effectively to unknown data while simultaneously reducing overfitting problems.

Model selection

Sequential CNN, as the pre-trained model for the classification of images, is utilized. For large dataset classification tasks, the CNN architecture has shown excellent performance. It easily identifies complex details in images.

Transfer learning

This method utilizes the trained CNN model as a feature extractor to take advantage of transfer learning. In this, the first layers' weights are frozen and only the subsequent layers' weights are adjusted to make them particular to the lumpy skin disease dataset. This methodology takes advantage of the depth of knowledge that the model has gained from a large dataset while conserving training time and processing resources. The procedure followed for the CNN model is presented in Fig 2.

Model architecture

The defined CNN model is designed for binary classification with two classes. The model architecture included six convolutional layers (Conv2D) with increasing filter sizes (32, 64) and kernel sizes (3×3), followed by max-pooling layers (MaxPooling2D) for spatial downsampling. After flattening the feature maps, the network runs data via a dense layer (Dense) activated by ReLU and 64 units. The output probabilities for each class are then generated by a dense layer using softmax activation. The architecture focuses on obtaining features through convolutional layers and records non-linear correlations in fully connected layers, following a standard pattern for image classification. Certain hyperparameters, such as layer depths and filter sizes, may require fine-tuning depending on the dataset's properties. The important architecture and training parameters of the CNN used in this study are listed in Table 2.

Six convolutional layers build up the sequential CNN architecture and each one uses 32 or 64 filters to extract complex characteristics from the input data. Six max-pooling layers are added to the design to efficiently down-sample spatial dimensions. A regularization strategy called dropout is employed strategically at a rate of 0.5 to improve the

Table 2: Convolutional neural network (CNN) hyperparameters.

Parameter	Description
Image size	256×256 pixels
Conv (2D) layer	6 (32 and 64)
Max pooling (2D) layer	6 (2×2)
Dropout rate	0.5
Function of activation	"Relu"
Epochs	50
Size of batch	32
Learning rate	0.0001

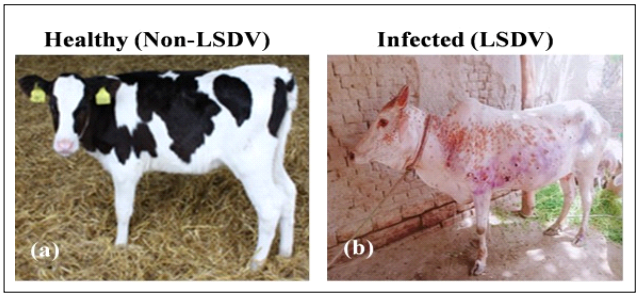

Fig 1: (a) Healthy (b) infected with LSDV.

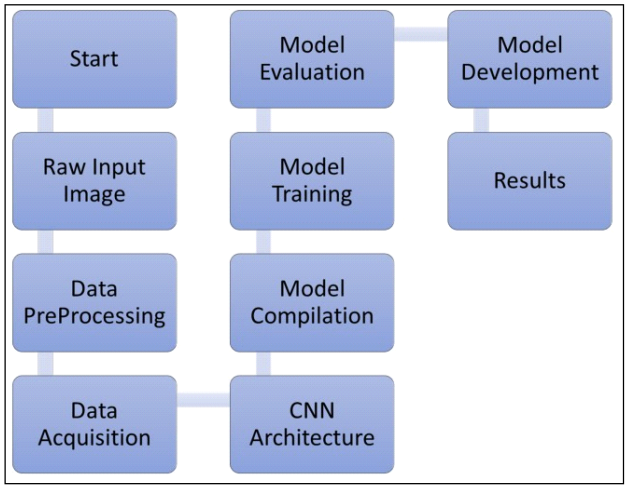

Fig 2: Procedure followed for the CNN model.

model's performance for generalization. The network is stable because of its uniform weight assignment, Rectified Linear Unit (ReLU) activation function and modest learning rate of 0.0001. The training protocol consists of 75 epochs with a batch size of 32 examples. Fig 3 shows the sketch of the overall architecture.

The process for the CNN model can be briefly described as follows. It involves processing the input image denoted as (x, y), with dimensions N × M, where (x, y) belongs to the set of real numbers. Equation 1 is used to compute the histogram of the image.

$$h_f(k) = 0j \quad ...(1)$$

Where:
$h_f(k)$= Histogram of an image.
f= Frequency of events.
O_j [j = 1, 2, 3…. (k-1)] = Events of grayscales.

Using the above formula, the range of infected images are given using equation 2:

$$\sim h_f(k) = h_f(k)[I_j]\ k_1, k_n \quad ...(2)$$

Where:
J = Pixel values.
I = Affected area.
k_1 to k_n = Range of the infected region.
$\sim h_f(k)$ = Complete infected region.

The total image variable negatives are determined using equation 3 and 4.

$$\sigma = \frac{1}{MN} \sum_{i=0,\ j=0}^{N-1,\ M-1} (\xi ij)^2 - \mu^2 \quad ...(3)$$

$$\mu = \sum_{i=0,\ j=0}^{N-1,\ M-1} (\xi ij) \times \frac{1}{MN} \quad ...(4)$$

The weight matrix and bias matrix of the convolutional layer are shown in equation 5 as follows:

$$S = \sum \xi xy + w + b \quad ...(5)$$

Where:
W = Weight matrix of the Ith layer.
b = Bias matrix of the Ith layer.
S = Properties of the first convolutional layer.
x, y = An enhanced image.

Next, the ReLu activation layer was added. The filter size of the subsequent convolutional layer was [3, 3], the stride was [1, 1] and there were 64 channels and 64 filters. ReLU activation function was used to normalize this layer's properties. A max-pooling layer with a filter size of [2, 2] and a stride of [2, 2] was then applied. The process is compiled using six convolutional and maxpooling layers, dropout, flatten and dense layer.

Evaluation matrices

To evaluate the model's performance, various metrics, including F1-score, Accuracy, Recall and Precision are determined. Based on the quantity of true positive (TP), true negative (TN), false positive (FP) and false negative (FN) samples, these metrics are calculated.

Accuracy

The ratio of correctly identified tests (positive or negative) to the total number of samples is known as accuracy.

$$\text{Accuracy \%} = \frac{TP + TN}{TP + TN + FP + FN} \times 100$$

Precision

Precision, which is defined as the ratio of correct positive predictions to all positive predictions made, is a statistic used to quantify the number of correct positive predictions built.

$$\text{Precision \%} = \frac{TP}{TP + FP} \times 100$$

Recall

The amount of accurate positive predictions made out of all possible positive predictions is measured using a metric called recall.

$$\text{Recall \%} = \frac{TP}{TP + FN} \times 100$$

F1 -Score

A single metric called the F-score is utilized to sum up model performance. When one of the matrices is high and the other is low, it can be utilized to balance out the model's performance.

$$\text{F1-score} = \frac{2 \times \text{Precision} \times \text{Recall}}{\text{Recall} + \text{Precision}}$$

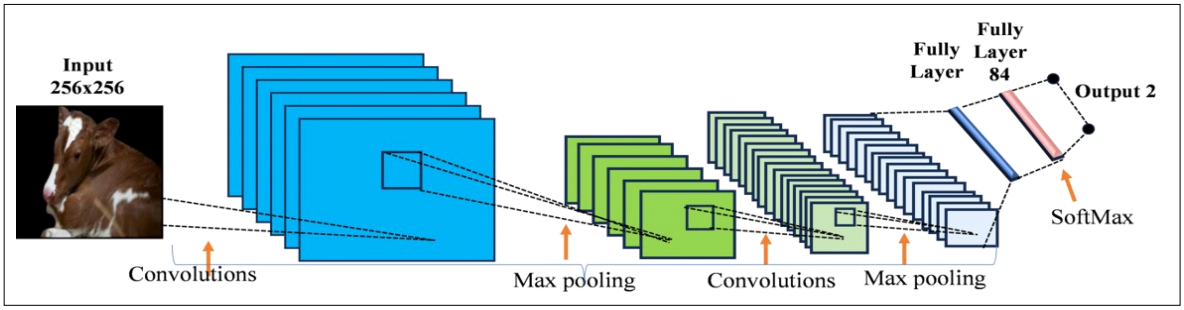

Fig 3: Architecture of model having convolution, pooling layers, flatten and dropout layers.

RESULTS AND DISCUSSION

In this study, a stack of convolutional layers to collect structural information and fully linked layers for classification illustrates a typical CNN approach for image classification. The architecture of the model uses max-pooling layers to gradually lower spatial dimensions, allowing the network to learn stacked representations of the input images. Class probabilities are output by the last dense layer using the softmax activation function. It's important to note that the model's performance is dependent on several variables, including the dataset's characteristics, the hyperparameters selected and the particulars of the classification task. For best results, experimentation and fine-tuning with various architectures and parameters could be required. The model is trained for 50 epochs, meaning it goes through the entire training dataset 50 times during training.

The accuracy of training and validation datasets is shown in Fig 4(a) and the corresponding loss values are shown in Fig 4(b). After the 50 epochs, the final accuracy on the training dataset is reported as 0.8654, meaning that the model correctly classified 86.54% of events in the test dataset. The average loss over the training dataset (after 50 epochs) is 0.7323. These metrics are often utilized to measure a machine learning model's performance on a held-out dataset and offer details on how well the model generalizes to new data.

To classify the images into actual and predicted levels, the prediction of cases belonging to a given class, such as Lumpy Skin, is presented in Fig 5. Actual lumpy skin, predicted lumpy skin and confidence 79.13% includes essential parts of the predictive model's output. Actual Lumpy Skin denotes the true label of the given instance. Predicted Lumpy skin is the output produced by the model that represents the algorithm's inference about the class identity of the instance that is being examined. The confidence score value (79.13%) represents the measured confidence level of the model in its prediction.

The metrics, including F1-score, recall and precision, are used to evaluate the CNN Model's performance. The confusion matrix for each class is shown in Fig 6.

The confusion matrix is a 2×2 matrix that shows the performance of a classification model performed on a binary classification test that had two classes: Normal Skin and Lumpy Skin. A classification model's correctness can be determined by analyzing its performance using specific measures. Lumpy Skin was accurately predicted by the

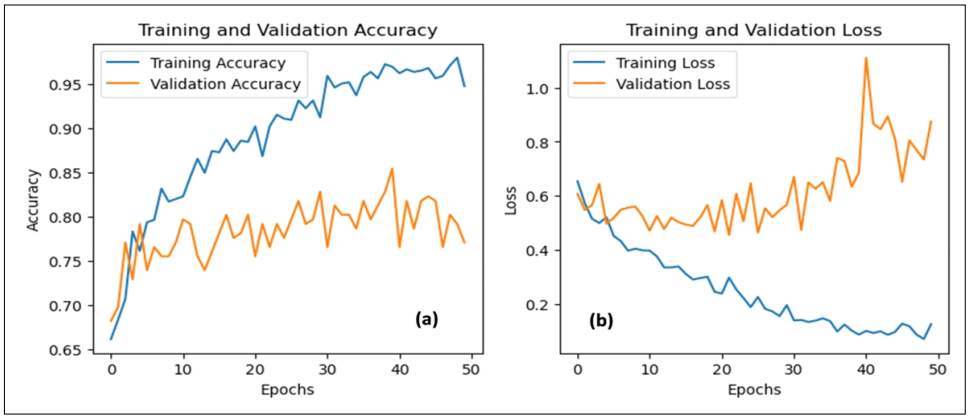

Fig 4: Accuracy and loss of training and validation dataset.

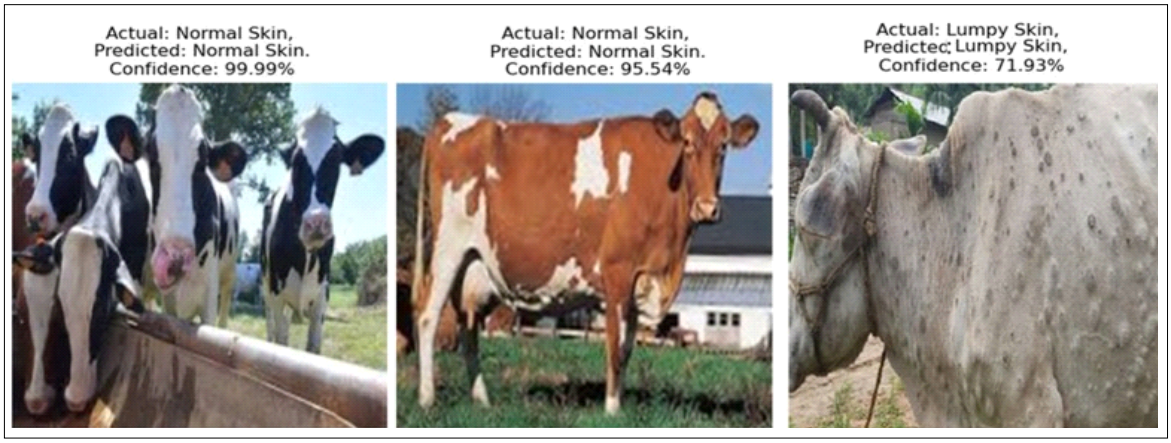

Fig 5: Actual, predicted classes with confidence score.

model nine times, as indicated by True Positives (TP). 24 incidents of the model incorrectly classifying Normal Skin as Lumpy Skin are known as False Positives (FP). False Negatives (FN) on the other hand, represent cases where Lumpy Skin has been mistakenly classified as Normal Skin (23 cases). True Negatives (TN) denote cases where the model successfully predicted Normal Skin (48 instances). These metrics together reveal the model's ability to differentiate between Lumpy Skin and Normal Skin, with TP and TN denoting accurate predictions and FP and FN indicating regions where the model's precision and recall might be improved.

The classification report (Table 3) gives a complete assessment of a model's performance in separating between Lumpy Skin and Normal Skin classes. The precision of Normal Skin is 0.74, showing a higher precision in recognizing occurrences of Normal Skin, compared to 0.45 for Lumpy Skin, which represents the accuracy of positive predictions. The model's recall, which measures its ability to record every relevant event, is 0.76 for Normal Skin and 0.42 for Lumpy Skin. The F1-score, which is a single statistic that combines recall and precision, is 0.75 for Normal and 0.44 for Lumpy Skin. With a weighted average F1-score of 0.65, the model's overall accuracy is 0.65. A balanced assessment across classes is suggested by the macro-average F1-score of 0.59. However, in some classes, the model did slightly better than in others. There could be a lot of reasons for this, including the quantity of images in each class and the fundamental challenge of differentiating between them.

Table 3: Classification parameter of disease prediction using CNN model.

	Precision	Recall	F1-score	Support
Lumpy skin	0.45	0.42	0.44	33
Normal skin	0.74	0.76	0.75	71
Accuracy			0.65	104
Macro Avg	0.60	0.59	0.59	104
Weighted Avg.	0.65	0.65	0.65	104

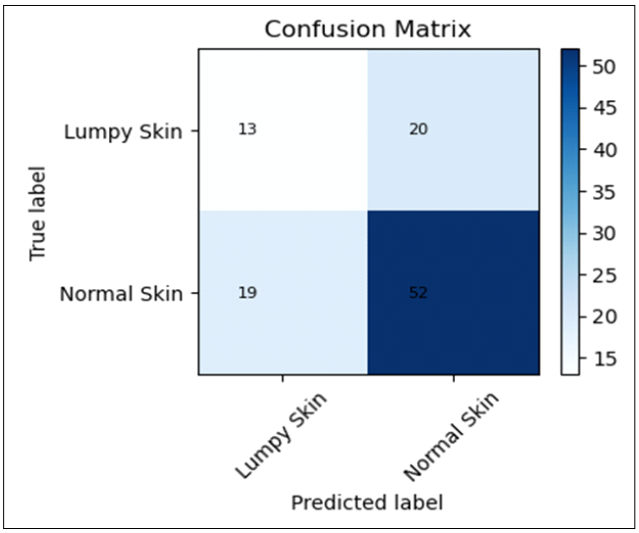

Fig 6: Confusion matrix.

The current investigation, in conjunction with prior studies, demonstrates the promising outcomes attained through the application of CNN in diagnosing skin diseases. Nevertheless, a notable challenge arises when working with images captured by mobile devices or digital cameras, as CNN models are not uniformly scaled and rotation invariant. Consequently, the accuracy of diagnostic results may be compromised if the image is not captured at the appropriate angle or orientation, hindering the attainment of consistent and reliable outcomes. Subsequent research efforts are imperative to tackle this challenge and enhance the performance of CNN models in the diagnosis of skin diseases.

With the comparison of the presented study, Jain *et al.* (2022) developed an OP-DNN for human skin disease classification, achieving 95% accuracy. Mellores *et al.* (2020) used ML to detect dog skin diseases like yeast and ringworm. An Android app developed using OpenCV and ANN models achieved 97% and 98% prediction accuracy, respectively. Afshari Safavi (2022) used meteorological and geological factors to assess the effectiveness of machine learning algorithms in predicting LSDV infection. The Extra Trees Classifier algorithm showed remarkable accuracy of up to 97%, outperforming other machine learning methods.

CONCLUSION

The study highlights the use of image processing and machine learning techniques in the detection of animal lumpy skin disease. A Convolutional neural network (CNN) for skin disease classification and detection is explained. The digital image processing using CNN, follows a set protocol that consists of image dataset collection, preprocessing, representation, interpretation and detection. This involves specific tasks such as ordering of channel, normalization, resizing images and data augmentation. The constructed classifier is evaluated by determining its robustness using measures like recall, accuracy, precision and F1-score. Precision and recall measures evaluate how accurately the model predicts each class in the context of this Lumpy Skin Disease study. The classification report evaluates a model's performance in distinguishing between Lumpy Skin and Normal Skin classes. Normal Skin has a higher precision of 0.74, while Lumpy Skin has a lower accuracy of 0.45. The model's recall and F1-score are 0.76 and 0.42, respectively, with a weighted average F1-score of 0.65. The model's accuracy in classifying instances within the designated classes is confirmed by the combined use of all these metrics. Its potential for real-world applications is highlighted by its insightful analysis of its overall effectiveness. To improve the model's effectiveness, experiments using a larger dataset, regularization and hyperparameter optimization, advanced image preparation methods and further

experimentation on feature extraction and categorization are needed. In-depth examinations of animal skin problems are also crucial for understanding cardiovascular health.

ACKNOWLEDGEMENT

The authors would like to thank the editors and reviewers for their review and recommendations and also to extend their thanks to King Saud University for funding this work through the Researchers Supporting Project number (RSP2024R395), King Saud University, Riyadh, Saudi Arabia.

Funding statement

This work was supported by the Researchers Supporting Project number (RSP2024R395), King Saud University, Riyadh, Saudi Arabia.

Author contributions

The author contributed toward data analysis, drafting and revising the paper and agreed to be responsible for all aspects of this work.

Data availability statement

Not applicable.

Declarations

Author(s) declare that all works are original and this manuscript has not been published in any other journal.

Conflict of interest

The author declare that they have no conflict of interest.

REFERENCES

Affolter, V.K., Yager, J.A., von Tscharner, C. and Mauldin, E. (2023). Pattern analysis for the diagnosis of inflammatory skin lesions in domestic animals: An overview. Veterinary Pathology. 60(6): 723-731. https://doi.org/10.1177/03009858231189456.

Afshari Safavi, E. (2022). Assessing machine learning techniques in forecasting lumpy skin disease occurrence based on meteorological and geospatial features. Tropical Animal Health and Production. 54(1): 55. https://doi.org/10.1007/s11250-022-03073-2.

AlZubi, A.A. (2023). Artificial intelligence and its application in the prediction and diagnosis of animal diseases: A review. Indian Journal of Animal Research. 57(10): 1265-1271. https://doi.org/10.18805/IJAR.BF-1684.

Amin, S.E., Haq, N.U., Haider, S., Shaukat, M.F., Arif, A., Fareed, A., Khan, A., Mehmood, A., Qammer, S. (2021). Emergence and transboundry spread of lumpy skin disease in South Asian Countries: A review. Journal of Xi'an Shiyou University, Natural Science. 18(9): 517-545.

Baselli, S., Pezzoni, G., Sabino, M., Grazioli, S., Wolff, J.W., Hoffmann, B., Shtjefni, V., Capucci, L. and Brocchi, E. (2023). ELISA methods based on monoclonal antibodies for the serological diagnosis of lumpy skin disease. Transboundary and Emerging Diseases. pp 1-13. https://doi.org/10.1155/2023/8378153.

Bekele, E. (2017). Pre-and post-slaughter factors that influence hide and skin quality in selected districts of West Shewa Zone, Oromia (Doctoral dissertation, Haramaya University).

Cho, O.H. (2024). An evaluation of various machine learning approaches for detecting leaf diseases in agriculture. Legume Research. https://doi.org/10.18805/LRF-787.

Datten, B., Chaudhary, A.A., Sharma, S., Singh, L., Rawat, K.D., Ashraf, M.S., Alneghery, L.M., Aladwani, M., Rudayni, H.A., Dayal, D., Kumar, S. and Chaubey, K.K. (2023). An extensive examination of the warning signs, symptoms, diagnosis, available therapies and prognosis for lumpy skin disease. Viruses. 15(3): 604. https://doi.org/10.3390/v15030604.

Dofadar, D.F., Abdullah, H.M., Khan, R.H., Rahman, R. and Ahmed, M.S. (2022). A comparative analysis of lumpy skin disease prediction through machine learning approaches. 2022 IEEE International Conference on Artificial Intelligence in Engineering and Technology (IICAIET). https://doi.org/10.1109/iicaiet55139.2022.9936742.

Gari, G., Biteau-Coroller, F., LeGoff, C., Caufour, P. and Roger, F. (2008). Evaluation of indirect fluorescent antibody test (IFAT) for the diagnosis and screening of lumpy skin disease using Bayesian method. Veterinary Microbiology. 129(3-4): 269-280. https://doi.org/10.1016/j.vetmic. 2007.12.005.

Genemo, M. (2023). Detecting high-risk area for lumpy skin disease in cattle using deep learning feature. Advances in Artificial Intelligence Research. 3(1): 27-35. https://doi.org/10.54569/aair.1164731.

Gupta, T., Patial, V., Bali, D., Angaria, S., Sharma, M. and Chahota, R. (2020). A review: Lumpy skin disease and its emergence in India. Veterinary Research Communications. 44: 111-118. https://doi.org/10.1007/s11259-020-09780-1.

Hosakoti, R., Kumar, S.P. and Jain, P. (2021). Disease detection in fruits using deep learning. J Univ Shanghai Sci Technol. 23(07): 309-312. https://doi.org/10.51201/JUSST/21/07125.

Jain, A.K., Tiwari, R.G., Ujjwal, N. and Singh, A. (2022). An Explainable Machine Learning Model For Lumpy Skin Disease Occurrence Detection. In 2022 International Conference on Data Analytics for Business and Industry (ICDABI) (pp. 503-508). IEEE. https://doi.org/10.1109/ICDABI56818.2022.10041665.

Johnson, A.E.W., Pollard, T., Berkowitz, S.A., Greenbaum, N.R., Lungren, M.P., Deng, C., Mark, R.G. and Horng, S. (2019). MIMIC-CXR, a de-identified publicly available database of chest radiographs with free-text reports. Scientific Data. 6(1). https://doi.org/10.1038/s41597-019-0322-0.

Kadian, S., Kumari, P., Shukla, S. and Narayan, R. (2023). Recent advancements in machine learning enabled portable and wearable biosensors. Talanta Open. 8: 100267. https://doi.org/10.1016/j.talo.2023.100267.

Kumar, V., Chaturvedi, V., Lal, B. and Alam, S. (2023). Application of Machine Learning in Analyzing the Psychological Well Being amongst the Employees in the Private Sector. An Analysis of Work-Life Balance in the Healthcare Industry. Pacific Business Review (International). 16(1): 124-131.

Li, Y., Deng, F., Hall, T., Vesey, G. and Goldys, E.M. (2021). CRISPR/Cas12a-powered immunosensor suitable for ultra-sensitive whole Cryptosporidium oocyst detection from water samples using a plate reader. Water Research. 203: 117553. https://doi.org/10.1016/j.watres.2021.117553.

Maltare, N.N., Sharma, D., Patel, S. (2023). An exploration and prediction of rainfall and groundwater level for the district of Banaskantha, Gujarat, India. International Journal of Environmental Sciences. 9(1): 1-17. https://www.theaspd.com/resources/v9-1-1-Nilesh%20N.%20Maltare.pdf.

Mellores, R.M.M., Salvoza, J.C.D., Flores, S.O., Arroyo, J.C.T. and Delima, A.J.P. (2020). Android-based Application Utilizing Image Processing with Artificial Neural Network for Detecting Ringworm and Yeast Infections for Dogs Using Neuroph Framework. International Journal. 9(3). https://doi.org/10.30534/ijatcse/2020/130932020.

Moriello, K.A. (2022). Diagnosis of Skin Diseases in Animals. MSD Manual. https://www.msdvetmanual.com/integumentary-system/integumentary-system-introduction/diagnosis-of-skin-diseases-in-animals [Accessed on 19/01/2024].

Nachbar, F., Stolz, W., Merkle, T., Cognetta, A.B., Vogt, T., Landthaler, M., Bilek, P., Braun Falco, O. and Plewig, G. (1994). The ABCD rule of dermatoscopy. Journal of the American Academy of Dermatology. 30(4): 551-559. https://doi.org/10.1016/s0190-9622(94)70061-3.

Neethirajan, S. and Kemp, B. (2021). Digital livestock farming. Sensing and Bio-Sensing Research. 32: 100408. https://doi.org/10.1016/j.sbsr.2021.100408.

Rashid, M.I., Rashid, M.I., Akbar, H., Ahmad, L., Hassan, M.F., Ashraf, K., Saeed, K. and Gharbi, M. (2018). A systematic review on modelling approaches for economic losses studies caused by parasites and their associated diseases in cattle. Parasitology. 146(2): 129-141. https://doi.org/10.1017/s0031182018001282.

Rojas-Anaya, E., Cantú-Covarrubias, A., Álvarez, J.F.M. and Loza-Rubio, E. (2016). Detection and phylogenetic analysis of bovine papillomavirus in cutaneous warts in cattle in Tamaulipas, Mexico. Canadian Journal of Veterinary Research. 80(4): 262-268.

Salvi, M., Acharya, U.R., Molinari, F. and Meiburger, K.M. (2021). The impact of pre-and post-image processing techniques on deep learning frameworks: A comprehensive review for digital pathology image analysis. Computers in Biology and Medicine. 128: 104129. https://doi.org/10.1016/j.compbiomed.2020.104129.

Scott, DW. (2018). 7 - Skin Diseases, Rebhun's Diseases of Dairy Cattle. [(Eds): Simon F. Peek, Thomas J. Divers], (3rd) Elsevier. (pp. 357-388). https://doi.org/10.1016/B978-0-323-39055-2.00007-3.

Sharawi, S.S.A. and Abd El-Rahim, I.H.A. (2011). The utility of polymerase chain reaction for diagnosis of lumpy skin disease in cattle and water buffaloes in Egypt. Revue Scientifique et Technique-OIE. 30(3): 821. https://doi.org/10.20506/rst.30.3.2075.

Srinivasu, P.N., SivaSai, J.G., Ijaz, M.F., Bhoi, A.K., Kim, W. and Kang, J.J. (2021). Classification of skin disease using deep learning neural networks with MobileNet V2 and LSTM. Sensors. 21(8): 2852. https://doi.org/10.3390/s21082852.

Tageldin, M.H., Wallace, D B., Gerdes, G.H., Putterill, J.F., Greyling, R.R., Phosiwa, MN., Busaidy, R.M.A. and Ismaaily, S.I.A. (2014). Lumpy skin disease of cattle: An emerging problem in the Sultanate of Oman. Tropical Animal Health and Production. 46(1): 241-246. https://doi.org/10.1007/s11250-013-0483-3.

Tupparainen, E., Alexandrov, T. and Beltran-Alcrudo, D. (2017). Lumpy skin disease: A field manual for veterinarians. Food and Agriculture Organization of the United Nations.

Vidic, J., Manzano, M., Chang, C.M. and Jaffrezic-Renault, N. (2017). Advanced biosensors for detection of pathogens related to livestock and poultry. Veterinary Research. 48(1): 1-22. https://doi.org/10.1186/s13567-017-0418-5.

Whittle, L., Chapman, R. and Williamson, A. L. (2023). Lumpy Skin Disease-An Emerging Cattle Disease in Europe and Asia. Vaccines. 11(3): 578. https://doi.org/10.3390/vaccines11030578.

Wasik, S. and Pattinson, R. (2024). Artificial Intelligence Applications in Fish Classification and Taxonomy: Advancing Our Understanding of Aquatic Biodiversity. FishTaxa. 31: 11-21.

Xiong, Y., Cao, G., Chen, X., Yang, J., Shi, M., Wang, Y., *et al.* (2022). One-pot platform for rapid detecting virus utilizing recombinase polymerase amplification and CRISPR/Cas12a. Applied Microbiology and Biotechnology. 106(12): 4607-4616. https://doi.org/10.1007/s00253-022-12015-9.

Zeedan, G.S.G., Mahmoud, A.H., Abdalhamed, A.M., Abd El, K.A.E.H., Khafagi, M.H. and Abou Zeina, H.A.A. (2019). Detection of lumpy skin disease virus in cattle using real-time polymerase chain reaction and serological diagnostic assays in different governorates in Egypt in 2017. Veterinary World. 12(7): 1093. https://doi.org/10.14202/vetworld.2019.1093-1100.